Available online at www.sciencedirect.com
SCIENCE DIRECT
Talanta 68 (2006) 623–628
Talanta
www.elsevier.com/locate/talanta

Uranium colloid analysis by single particle inductively coupled plasma-mass spectrometry

C. Degueldre [a,*], P.-Y. Favarger [b], R. Rossé [a], S. Wold [c]

[a] *Department Nuclear Energy and Safety, Paul Scherrer Institut, 5232 Villigen-PSI, Switzerland*
[b] *Institut Forel, University of Geneva, 1290 Versoix, Switzerland*
[c] *Department of Chemistry, Royal Institute of Technology, Stockholm, Sweden*

Received 20 December 2004; received in revised form 2 May 2005; accepted 2 May 2005
Available online 23 June 2005

Abstract

Uranium single particle analysis has been performed by inductively coupled plasma-mass spectrometry (ICP-MS) and the performances are compared with that provided by scanning electron microsopy and single particle counting. The transient signal induced by the flash of ions due to the ionisation of an uranium colloidal particle in the plasma torch can be detected and measured for selected uranium ion masses ($^{238}U^+$, $^{235}U^+$ or $^{254}[^{238}U^{16}O]^+$) by the mass spectrometer. The signals recorded via time scanning are analysed as a function of particle size or fraction of the studied element or isotope in the colloid phase. The frequency of the flashes is directly proportional to the concentration of particles in the colloidal suspension. The feasibility tests were performed on uranium dioxide particles. The study also describes the experimental conditions and the choice of mass to detect uranium colloids in a single particle analysis mode.

Keywords: Single particle analysis; Inductively coupled plasma-mass spectrometry; Uranium particle; Particle size; Isotope

1. Introduction

Single particle analysis from a suspension is generally performed after separation by scanning electron microscopy (SEM) investigation on a filter [1]. Single particle analysis has been performed over a decade utilising light-based techniques, such as optical single particle counting (SPC) [2] or laser induced breakdown detection [3]. These techniques have been applied to the analysis of natural water [4,5], loop or reactor water [6,7]. The conventional inductively coupled plasma-atomic emission spectrometry (ICP-AES) was successfully adapted by Borchet [8] for individual particle analysis. Mass spectrometry (MS) is one of the primary analysis methods for determining the chemical composition of small samples, consequently several of these techniques have been adapted to analyse single aerosol particles [9]. After separation on a specific sample carrier, laser microprobe mass analysis (MS) can be applied for single particle analysis [10].

The utilization of inductively coupled plasma-mass spectrometry (ICP-MS) for single particle analysis was first discussed for colloid bearing solutions by the author in [1]. Independently, Nomizu et al. [11,12] successfully tested this approach for airborne particles at the fg level. Recently, the feasibility of single particle analysis on TiO_2, Al_2O_3, clay colloids [13], ZrO_2 colloids [14] and ThO_2 colloids [15] from suspension in water was studied by ICP-MS. These recent studies concerned colloids and determination of size resolution limit (<100 nm).

In this work, single particle ICP-MS analysis was tested for uranium dioxide particles in diluted suspensions. The signal induced by the ionisation of a uranium loaded particle in the plasma torch produces a flash of uranium ions that can be detected and measured by the mass spectrometer. This study focusses on uranium oxide particles (0.1–10.0 μm) because when their size is greager than a few micrometres the MS detector can be saturated and shut down for detector safety,

* Corresponding author. Tel.: +41 56 3104176; fax: +41 56 3104595.
E-mail address: claude.degueldre@psi.ch (C. Degueldre).

0039-9140/$ – see front matter © 2005 Elsevier B.V. All rights reserved.
doi:10.1016/j.talanta.2005.05.006

stopping the analysis. This uranium particle specific work may be of concern for several case studies, e.g. reactor water [16], solutions loaded with pellet fragments, yellow cake colloidal particles for exemple produced by a redox front [17,18] and particles contamined with uranium [19]. This study may be adapted to analyse uranium doped particles in surface or shallow waters, suspensions of milled uranium dioxide samples difficult to leach in acid, or environmental samples contaminated with particles yield after impact of perforation rocked heads.

2. Theoretical background

In single particle mode, the ICP-MS is adapted for the injection of individual particles in the water stream during each analysis time slot of the MS. Colloids are continuously introduced in the nebulizer producing an aerosol of micro-drops (some containing a colloid at a time) feeding the inductively coupled plasma torch connected to a mass spectrometer. With this system, the particles are ionized up to a limited size in the plasma torch with a maximum frequency of one per recorded time slot.

A colloid suspension of formula MO_x (molecular weight M_{MOx} [g mol^{-1}]) and of colloid concentration N_{col} (cm^{-3}) is injected at a flow rate q_{col} (cm^3 s^{-1}) in the stream of a blanc water with a flow rate of q_{sol} (cm^3 s^{-1}) if needed. The diluted suspension is sprayed with a nebulisation yield η_{neb} (−) and transported in the argon flow q_{Ar} (cm^3 s^{-1}) into the plasma torch. The plasma temperature T_p (K) allows the gas to undergo an isobaric expansion from room temperature, e.g. 300 K to T_p, with T_p/300 usually of ∼20 [20]. Each single particle undergoes an ionisation and the flash of generated ions is a function of the size of the initial particle d_{col} (cm) with the flash frequency, f (s^{-1}), a direct function of the colloid concentration N_{col} (cm^{-3}). A fraction η_A (−) of the isotope ions $^AM^+$ ($\eta_A = \eta_{A(t)}\ \phi_A\ \phi^+$ with ϕ_A the isotopic fraction of ^AM, with ϕ^+ the fraction of M^+), produces an ion single flash that passes through the cone hole and that can be detected by the mass spectrometer detector with a counting yield η_c (−). However, M^{j+} ions (with $1 \leq j \ll Z$, with Z the atomic number of M), and with $\eta_{A(t)}$ the fraction of elemental ion M^{j+} may also be produced from MO_x, together with other ions (MO^+, $MO^{2+}\cdots$, $MO_2{}^+, \cdots$). The signal observed for a given ion mass as a function of time is a peak whose intensity is a function of the mass of the analyzed colloid and the fraction of the element and/or isotope in the colloid considered. The number of M ions N_M (−) for a single MO_x particle of size d_{col} (cm) is given by:

$$N_M = \frac{\pi d_{col}^3 \rho N_{Av}}{6 M_{MO_x}} \quad (1)$$

where ρ (g cm^{-3}) is the colloid density and N_{Av} the Avogadro constant (mol^{-1}). The ions from the solid colloid that originally explodes in the torch generate $MO_2{}^{i+}, \cdots MO^+, \cdots M^{j+}$ and $^AM^+$; only the latter however is generally detected. An $^AM^+$ ion fraction passes through the spectrometer and the signal s_A (s^{-1}) is detected for the isotope ion $^AM^+$ or its interferences, e.g. $^{2A}M^{*2+}$ or $[^{A-z}M^{\#z}Z]^+$ as a function of time. The number of molecules of MO_x is deduced from the number of M atoms N_M, which is deduced from the signal s_A by the expression:

$$s_A = \eta_A\ \eta_C\ N_M \quad (2)$$

Combining Eqs. (1) and (2) gives:

$$s_A = \xi\ d_{col}^3 \quad (3)$$

(with $\xi = \pi\eta_A\eta_C\rho N_{Av}/6M_{MOx}$) that may be used for the size distribution evaluation. However, the size of the largest particle to be ionized in the plasma torch has to be evaluated. The colloid concentration N_{col} in the original suspension is diluted by a factor q_{col}/q_{sol}. The fraction η_{neb} is found in argon. The colloid frequency detection f is then simply given by the product:

$$f = \eta_{neb}\ N_{col}\ q_{col} \quad (4)$$

The Eqs. (3) and (4) allow calculation of the metal size distribution (N_{col} versus d_{col}) in the colloid phase on the basis of the signal distribution (f versus s_A) or vice versa.

3. Experimental and material characterisation

The uranium dioxide stock fine was produced by manual milling of a UO_2 powder (Sweden Uran, today, Westinghouse) in an agate mortar. The initial uranium dioxide stock suspensions had a weight concentration of 2 mg in 50 ml water and contained widely poly-dispersed colloids. The suspensions were shaken manually for 2 min. The stock solution was diluted 100 times with MilliQ water.

The scanning electron microscopy (SEM) investigations were performed under 30 kV with a Zeiss DSM 962. SEM investigations on the 100–10,000 nm uranium oxide colloids were carried out with powder contacted onto double side sticking C-Tabs and coated with 15 nm Pt layer by Magnetron sputtering prior to microscopic investigation, see Fig. 1. The microscopic investigations on uranium oxide colloids revealed a broad size distribution, such as obtained by SPC.

Single particle counting investigations light scattering was carried out at 780 nm (30 mW solid state laser) for 90° and for 10 runs of 1 min duration. A single particle monitor (HSLIS-M50) and a single particle spectrometer (HVLIS-C200), both units from Particle Measuring Systems Inc. (PMS), Boulder, Colorado, were used on-line sequentially as described earlier [21]. The colloid solution is injected at a flow rate (q_{col}) 200 ml h^{-1} in the main stream of blanc water (of 500 ml min^{-1}) and which is then split in two with a q_{sol} of 100 ml min^{-1} for the M50 unit and 400 ml min^{-1} for the C200 unit. The size window limits that were used for the SPC analyses were: 50, 100, 150 and >200 nm for the M50

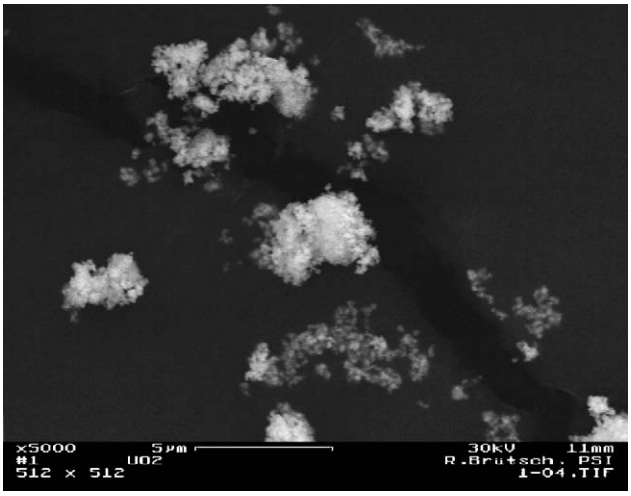

Fig. 1. Uranium dioxide colloid analysis by SEM.

unit, and 10 windows of 100 nm width from 200 to 1200 nm, followed by 200 nm windows to 2000 nm for the C200 unit.

SPC investigations by light scattering were carried out on the initial colloid suspensions for comparison. Their size distributions in the stock suspensions were determined. An average diameter can not be derived for the uranium dioxide colloids (see Fig. 2). The distribution function indicates a polydispersivity. The SPC results for both powders prepared by milling follow somewhat the expected Pareto power law:

$$\frac{\delta N_{\mathrm{col}}}{\delta d_{\mathrm{col}}} = A\, d_{\mathrm{col}}^{-b} \tag{5}$$

with the $\log N_{\mathrm{col}}$ versus $\log d_{\mathrm{col}}$ displaying an average slope with $b \sim 4$ [22]. These broad particle size distributions present, however, some particle classes around 100, 300 and more specifically around 750 nm. This last particle class (e.g. 750 ± 150 nm) is compared with the distribution measured for 802 ± 10 nm latex colloids (Nanosphere^{TM} starndard).

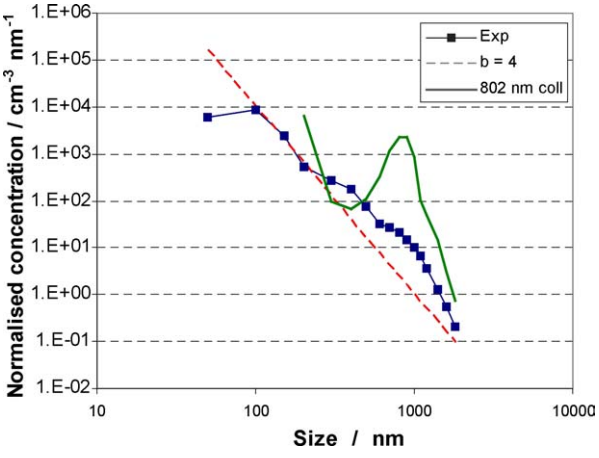

Fig. 2. Uranium colloid particle and volume distribution derived from SPC measurements. Conditions: uranium dioxide (UO_2) colloids, $q_{\mathrm{col}} = 2 \times 10^2\ \mathrm{cm^3\ h^{-1}}$, $q_{\mathrm{sol}} = 1 \times 10^2\ \mathrm{cm^3\ min^{-1}}$ (M50 unit) and $q_{\mathrm{sol}} = 4 \times 10^2\ \mathrm{cm^3\ min^{-1}}$ (C200 unit); legend: for Eq. (3) fit with $b = 4$, larger colloid fraction with a maximum population for $d_{\mathrm{col}} = 800$ nm.

The ICP-MS unit was a HP (Hewlett Packard) 4500 series 100. The flow rate of MilliQ blank water q_{sol} was $5.03 \times 10^{-3}\ \mathrm{cm^3\ s^{-1}}$. For analysis using ICP-MS, the target suspensions in MilliQ water contained colloid number concentrations of 10^5–$10^6\ \mathrm{cm^{-3}}$. The colloid suspension was introduced by a syringe driven by a linear motor. The colloid suspension injection rate q_{col} was $2.2 \times 10^{-5}\ \mathrm{cm^3\ s^{-1}}$. The argon, CARBA 4.8 (purity 99.998%), was provided from a reservoir filled with liquid argon. The flow rate of the carrier gas q_{Ar} was $19\ \mathrm{cm^3\ s^{-1}}$ and that for the internal and external coolants the flow rate was 16 and $150\ \mathrm{cm^3\ s^{-1}}$, respectively. The nebuliser was a Babbington^{TM} type. The injector was 1 mm in diameter and the torch sizes were: ~4 cm long and ~1 cm radius. The signals were recorded in time scan mode including a measurement window of 0.1 ms, followed by a standby period of 9 μs; the data included integration over a Δt of 10 ms with a corresponding standby. Currently, a scan of 2000 records corresponded to a period of about 20 s measurement and 0.18 s total standby. The standby periods (9 μs) allow the detector to recover.

4. ICP-MS results and discussion

ICP-MS measurements were carried out with diluted uranium dioxide colloid suspensions.

UO_2 colloids were detected for $^{238}U^+$ whose isotopic abundance ϕ_A is 99.275%. The potential isobaric interferences are $^{119}Sn_2{}^+$ or $^{238}Pu^+$, however, neither ^{119}Sn (8.59%) nor Pu was present in the solution and could be easily determined if present. Further, for large particles, interferences with $[^{A-z}M^{\#z}Z]^+$ for $z = 12$, 14, 16 and 40 would concern ^{226}Ra, short life radionuclides (mass 224 or 222) and ^{195}Pt, which are all currently absent from the suspension and could easily be detected if present. Fig. 3a shows a typical record of signals obtained for mass 238 (s_{238}) as a function of time. The signals are printed out every 10 ms, with a record of 2000 data points over 20 s. For the smaller colloids, the signal per 10 ms ranged from some counts to around 100 counts. The signal distribution for the particle class around 750 nm can be seen in Fig. 3b. The calculation of the signal distribution (f versus s_A) was carried out for $\xi = 10^{-5}\ \mathrm{nm^{-3}}$ an average d_{col} of 750, 300 and 160 nm and a standard deviation of 130, 50 and 90 nm for comparable data fit with the SPC result. The background for mass 238 was of 0 or 1 count/10 ms and the detection limit on the size of these colloids based on a 3 times the standard deviation of the background is ~80 nm. Since the studied colloids are 100–10,000 nm in size it is expected that their total atomisation takes place in the plasma up to a certain size. Consequently, an attention is carried out for rather large particles (around 4000 nm) that could also shut down the detector gate.

However, for large particles (e.g. larger than 5000 nm) their atomisation during flight in the plasma may be partial

only, consequently limiting the use of this approach. The evaluation of the particle sublimation time θ as a function of its size d_{col} was performed for an average thermal conductivity κ of 3 W m^{-1} K^{-1} in the temperature range between the ambient temperature T_0 and the plasma temperature T_p. The other thermodynamic parameters required for calculation are: the thermal capacity (c_P = 80 J mol^{-1} K^{-1}), molecular weight (M_{UO2} = 270 g mol^{-1}) and density of UO_2 (ρ = 11 g cm^{-3}). Calculations were carried out using a Green's function adapted for spherical geometry with size d_{col} without a phase change along the temperature range (T_0–T_f) and with complete sublimation at that temperature T_f. The relative temperature difference: $T_p - T_f/T_p - T_0$ may be plotted as a function of the parameter $(= 4D\theta/d_{col}^2$, where θ is the particle residence time in the plasma and D the thermal diffusivity of the particle material ($D = \kappa/(\rho\, c_p) = 25 \times 10^{-7}$ cm^2 s^{-1}). The plot, $\log[(T_p - T_f)/(T_p - T_0)] = -5.678\,(4D\,\theta/d_{col}^2) + \log 0.7$ is used to estimate the average temperature of the particle during its flight in the plasma. No sublimation or melting/boiling is supposed to take place at temperature lower than T_f to simplify the problem. Table 1 gives the results expressed in particle residence time as a function of their size to reach final temperature (T_f). It must be noted that in reality larger particles may sublimate since the peal-out of the particle starts at the very beginning of its residence time in the plasma. Recently, high-speed digital photography studies, e.g. [23] of micrometer size Y_2O_3 particles demonstrated that the velocity of the particles is the same for all sizes of particle (~30 m s^{-1} in standard ICP) and that their atomization may take place at the micrometre size level. It must be noted that Y_2O_3 is a conservative case since its Gibbs formation energy is the largest for the oxides.

Table 1
Evaluation of time θ required to reach an average particle temperature of 4200 K in a 7000 K plasma during a UO_2 particle flight in the plasma

Colloid size d_{col} (nm)	200	600	2000	6000	20,000
θ (s)	10^{-6}	10^{-5}	10^{-4}	10^{-3}	10^{-2}

Conditions: particle average speed: 100 m s^{-1}; note that in the utilised plasma torch the maximum residence time τ is around 10^{-3} s.

If 100 nm $^{238}UO_2$ colloids are analysed by ICP-MS they yield peaks of about 10 counts, the 1000 nm colloids

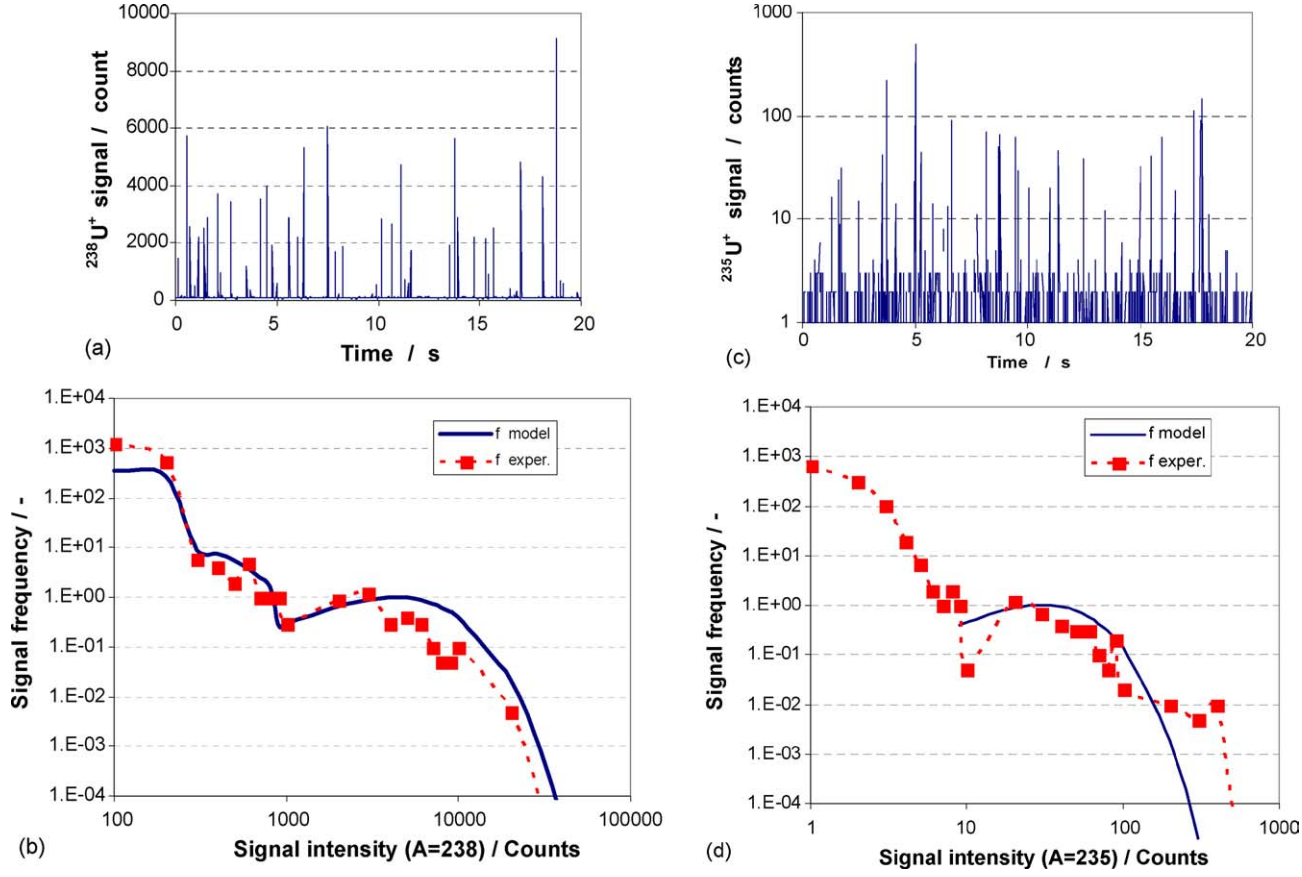

Fig. 3. Analysis of uranium dioxide (UO_2) colloids by ICP-MS in a single particle mode. (a): Signal s_{238} for $^{238}U^+$ recorded in time scan, particle sample recorded during 20 s, intensity in counts per 10 ms. (b): Signal analysis: $f(s_{238})$ versus s_{238}. Modeling conditions: $\xi = 10^{-5}$ nm^{-3} and 3 Gaussians: $d_{col} = 160 \pm 90$ nm, $d_{col} = 300 \pm 50$ nm and $d_{col} = 700 \pm 130$ nm with concentration given by Fig. 2. (c): Signal s_{235} for $^{235}U^+$ recorded in time scan, particle sample recorded during 20 s, intensity in counts per 10 ms. (d): Signal analysis: $f(s_{235})$ vs. s_{235}. Modeling conditions: $\xi = 10^{-7}$ nm^{-3} and Gaussian: $d_{col} = 700 \pm 130$ nm. (e): Signal s_{254} for $^{254}[UO]^+$ recorded in time scan, particle sample recorded during 20 s, intensity in counts per 10 ms. (f): Signal analysis: $f(s_{254})$ vs. s_{254}. Modeling conditions: $\xi = 6 \times 10^{-8}$ nm^{-3} and 1 Gaussian: $d_{col} = 700 \pm 130$ nm. Conditions: colloidal suspension of UO_2, 10 ms detection time for U ion detection, $q_{col} = 2 \times 10^{-5}$ cm^3 s^{-1}, $q_{sol} = 5 \times 10^{-3}$ cm^3 s^{-1}, $q_{Ar} = 19$ cm^3 s^{-1}.

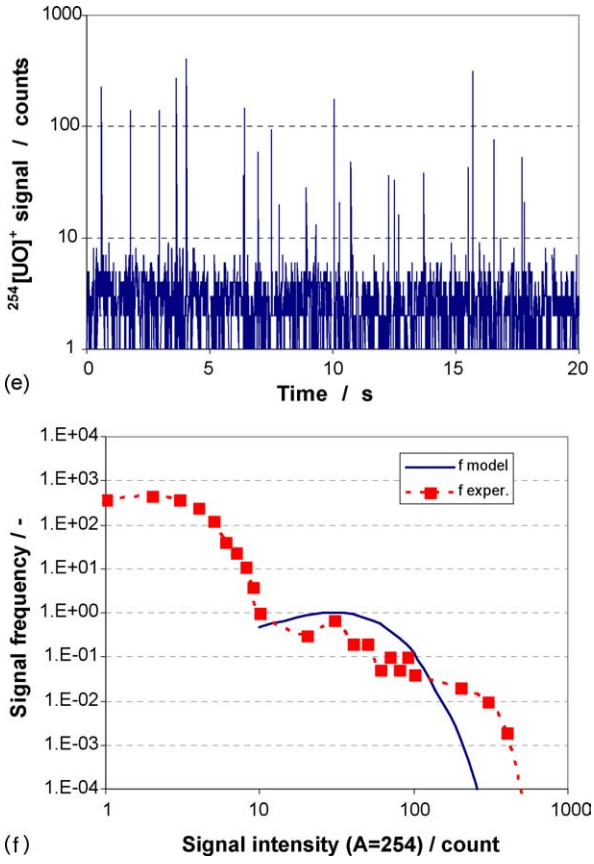

Fig. 3. (*Continued*).

would give 10×10^3 counts, the 2000 nm colloids would yield 8×10^4 counts and the 4000 nm colloids would yield 64×10^4 counts which could already shut-down the detector (e.g. for 10^5 counts).

Uranium dioxide particles may be tested for other masses to avoid shut-down of the detector. UO_2 colloids were subsequently analysed using mass 235 with isotope ^{235}U, whose isotopic abundance ϕ_{U235} is 0.72%. The isobaric interference $^{235}Pa^+$ does not have to be considered because of its short half-life. Further interferences for $[^{A-z}M^{\#z}Z]^+$ with $z = 12$, 14, 16 or 40 were absent. The background at mass 235 was found to be of 0–1 count/10 ms. The record given in Fig. 3c presents typical signals obtained for mass 235 (s_{235}). It may be compared to that registered for $^{238}U^+$ (s_{238}) and that recorded for $^{254}[^{238}U^{16}O]^+$ (s_{254}), see Fig. 3e. The distribution analysis (Fig. 3d) of the ICP-MS signals reveal the top of the signal analysis obtained for mass 238 corrected by a factor of about 130 (corresponding to the isotopic ratio). The signal distribution for the particle class around 750 nm presented in Fig. 3d was calculated for $\xi = 7.25 \times 10^{-8}$ nm^{-3} and the average d_{col} of 750 ± 130 nm for comparable data fit with the SPC result. Note that the detection of the mass 235 induces a change of scale for size class avoiding the shut down of the detector gate for large colloids. The isotopic abundance must however be assessed to quantify the distribution.

UO_2 colloids were finally analysed for the mass 254 of the $^{254}[^{238}U^{16}O]^+$ cluster ions, whose isotopic abundance $\phi_{235U16O}$ is 99.04%. The potential isobaric interferences for $[^{A+16-z}M^{\#z}Z^{16}O]^+$ with $z = 12$, 14 or 40 and M#: Pu, Ra and Fr, were absent. The background at mass 254 was found to be of 0–1 count/10 ms. The record given in Fig. 3e presents typical signals obtained for mass 254 (s_{254}). The distribution analysis (Fig. 3f) of the ICP-MS signals reveals the top of the signal analysis obtained for mass 254 corrected by a factor of about 150 (corresponding to the ratio between both isotopic abundances). Note that the change of scale for size class avoiding the shut down of the detector gate. The comparison of the distribution for the particles given for the detection at the masses 238, 235 and 254 (Fig. 3b, d and f) are comparable when corrected from the count ratio for the abundance of these ions. In order to test the cluster ion abundancy one test was with uranyl nitrate solution, and the counting rate was found to be: 29302 ± 745 counts for $^{238}U^+$, 206 ± 15 counts for $^{254}[^{238}U^{16}O]^+$ for 64 measurements. The signal distribution for the particle class around 750 nm presented in Fig. 3d was calculated for $\xi = 7.03 \times 10^{-8}$ nm^{-3} and the average d_{col} of 750 ± 130 nm for comparable data fit with the SPC result.

The colloids could also be analysed for the mass 251 corresponding to the ion $^{251}[^{235}U^{16}O]^+$, whose abundance $\phi_{235U16O}$ is ~0.72 %. However, the production yield of $^{251}[UO]^+$ being low, this cluster ion was not studied because it would correspond to particle sizes that are not expected to be fully atomized during their flight in the plasma torch.

The colloid size distribution analysis, which is currently carried out by SEM, may be performed together with their chemical characterisation by quantitative energy dispersive spectroscopy (EDS). However, these investigations require sample preparation, observation and particle counting, which is time consuming, e.g. 20 h. The utilization of SPC is much more rapid (e.g. 20 min) because it may be carried out on line, however this analysis provides numbers and sizes. The use of ICP-MS in a single particle mode makes the analysis (isotopic and size distribution) in 20 s possible, demonstrating the potential of this technique.

Acknowledgements

Part of the work was performed at Institute Forel which laboratory is partially supported by the Swiss National Foundation. The concept and modeling work was performed at LES-PSI partially funded by the National Cooperative for the Disposal of Radioactive Waste. Thanks are due to R. Brütsch for sample preparation and SEM investigation, at the Hot Laboratory, PSI and to J.L. Loizeau at Institute Forel for additional SPC tests.

References

[1] J. McCarthy, C. Degueldre, Characterisation of Environmental Particles, 2, Lewis Publishers, Chelsea, MI, 1993, pp. 247–315 (Chapter 6).

[2] C. Degueldre, H.-R. Pfeiffer, W. Alexander, B. Wernli, R. Brütsch, Appl. Geochem. 11 (1996) 677–695.
[3] T. Bundshuh, R. Knopp, R. Müller, J.I. Kim, V. Neck, Th. Fanghänel, Radiochim. Acta 88 (2000) 625–629.
[4] C. Degueldre, I. Triay, J.I. Kim, M. Laaksoharju, P. Vilks, N. Miekeley, Appl. Geochem. 15 (2000) 1043–1051.
[5] P. Steinmann, Th. Billen, J.-L. Loizeau, J. Dominik, Geochim. Cosmochim. Acta 63 (1999) 1621–1633.
[6] C. Degueldre, A. Bilewicz, H.P. Alder, Nucl. Sci. Eng. 120 (1995) 65–71.
[7] C. Degueldre, E. Schenker, H. Nobbenhuis-Wedda, in: Proceedings Conference on Water Chemistry of Nuclear Reactor Systems, vol. 7, publisher BNES, 1996.
[8] U.K. Borchet, W. Dannecker, J. Aerosol. Sci. 20 (1988) 1525–1528.
[9] C. Noble, K. Prather, Phys. World 11 (1998) 39–43.
[10] S.R. Biegalski, L.A. Currie, R.A. Fletcher, G.A. Klouda, R. Weissenbök, Radiocarbon 40 (1998) 3–11.
[11] T. Momizu, S. Kaneco, T. Tanaka, T. Yamamoto, H. Kawaguchi, Anal. Sci. 9 (1993) 843–846.
[12] T. Momizu, N. Hoshino, S. Kaneco, T. Tanaka, T. Yamamoto, H. Kawaguchi, K. Kitagawa, Anal. Sci. 17 (2001) 61–64.
[13] C. Degueldre, P.-Y. Favarger, Colloids Surf. A 217 (2003) 137–142.
[14] C. Degueldre, P.-Y. Favarger, C. Bitea, Anal. Chim. Acta 518 (2004) 137–142.
[15] C. Degueldre, P.-Y. Favarger, Talanta 62 (2004) 1051–1054.
[16] J.A. Kersten, J. Nucl. Energy 16 (1962) 15–18.
[17] E.C. Buck, P.A. Finn, J.K. Bates, Micron 35 (2004) 235–243.
[18] N. Miekeley, H. Countinho de Jesus, C.L. Porto da Silveira, C. Degueldre, J. Geochem. Explor. 45 (1992) 409–437.
[19] A.J. Dent, J.D. Ramsay, S.W. Swanton, J. Colloid Interface Sci. 150 (1992) 45–60.
[20] Mao Huang, D.S. Hanselman, Pengyuan Yang, G.M. Hieftje, Spectrochim. Acta 47B (1992) 765–785.
[21] C. Degueldre, A. Bilewicz, W. Hummel, J.L. Loizeau, J. Environ. Radioact. 55 (2001) 241–253.
[22] A. Lerman, Geochemical Processes, Water and Sediment Environments, Wiley, 1979.
[23] D.B. Aeschliman, S.J. Bajic, D.P. Balwin, R.S. Houk, J. Anal. At. Spectrom. 18 (2003) 1008–1014.